Preformed excitons, orbital selectivity, and charge density wave order in $1T$-$TiSe_2$

S. Koley,[1] M. S. Laad,[2] N. S. Vidhyadhiraja,[3] and A. Taraphder[1,*]

[1]*Department of Physics and Centre for Theoretical Studies, Indian Institute of Technology, Kharagpur 721302 India*

[2]*Max Planck Institute for Physics of Complex Systems, 38 Nöthinitzer Strasse, 01187 Dresden, Germany*

[3]*Theoretical Sciences Unit, Jawaharlal Nehru Centre for Advanced Scientific Research, Bangalore 560064 India*

(Received 2 May 2014; published 25 September 2014)

Traditional routes to charge density wave (CDW) in transition-metal dichalcogenides, relying on Fermi surface nesting or Jahn-Teller instabilities, have recently been brought into question. While this calls for exploration of alternative views, a paucity of theoretical guidance sustains lively controversy on the origin of, and interplay between, CDW and superconductive orders in transition-metal dichalcogenides. Here, we explore a preformed excitonic liquid route, heavily supplemented by modern correlated electronic-structure calculations, to an excitonic CDW order in $1T$-$TiSe_2$. We show that orbital-selective dynamical localization arising from preformed excitonic liquid correlations is somewhat reminiscent of states proposed for d and f band quantum criticality at the border of magnetism. Excellent quantitative explication of a wide range of spectral and transport responses in both normal and CDW phases provides strong support for our scenario, and suggests that soft excitonic liquid fluctuations mediate superconductivity in a broad class of transition-metal dichalcogenides on the border of CDW. This brings the transition-metal dichalcogenides closer to the bad actors (where the metallic state is clearly not a Fermi liquid) in d and f band systems, where anomalously soft fluctuations of electronic origin are believed to mediate unconventional superconductivity on the border of magnetism.

DOI: 10.1103/PhysRevB.90.115146 PACS number(s): 71.45.Lr, 71.30.+h, 75.50.Cc

I. INTRODUCTION

Twenty six years after the path-breaking discovery of high-T_c superconductivity in doped, quasi-two-dimensional (quasi-2D) copper oxides (cuprates), the list of poorly understood strongly correlated electronic systems with partially filled d or f bands continues to grow [1–3]. The paradigm shift engendered by cuprates also fueled renewed interest and study of older systems. Before the cuprate revolution, these were sore spots in the standard model of electrons in metals, centered around the celebrated Landau Fermi liquid (LFL) theory. Intense activity to unravel increasing variety of unconventional ordered states with unconventional metallicity has stabilized this paradigm shift. Cuprates are not, it is now clear, an isolated example: rare-earth systems close to magnetic instabilities at $T = 0$, increasing number of d band perovskites and the recent explosion in Fe-pnictides are but a few examples of a truly diverse zoo of strange systems.

Perhaps equally remarkable is the fact that careful work in the recent past has brought out unexpected similarities between the newer and older bad actors above. This is best exemplified by the recent revival of interest in quasi-2D transition-metal dichalcogenides (TMD). For more than 40 years, the origin of charge density wave (CDW) and superconductive (SC) orders and their interplay in the layered TMD had remained poorly understood issues [4,5]. Historically, appealing to one-electron (density functional theory) band structure led to the conventional wisdom of CDW arising from Fermi surface (FS) nesting, or via a band Jahn-Teller (JT) instability. There have also been suggestions of CDW or spin density wave (SDW) mediated pairing mechanisms, based on exchange of respective fluctuations over weak coupling ground states, in the context of bismuthates and cuprates [6,7]. Recent revival in the field was stimulated, among other things, by falsification of these weak coupling views in the context of dichalcogenides, by high-resolution ARPES work [8]. The exciting possibility of an alternative, intrinsically strong coupling view, involving CDW order emerging as a Bose-Einstein condensation (BEC) of an incoherent preformed excitonic liquid (PEL) normal state, arose [9–11] as an attempt to address this new conflict, and has the potential to bring TMD into the list of strange actors. Indeed, parallels between TMD and cuprates have increasingly been claimed in certain studies [12]. It is also suggested that the absence of magnetism in TMD allows studies of a bad metal without attendant magnetic fluctuations that complicate the physics in cuprates [13]. That a strong coupling scenario for TMD closer to the Mott limit is in order is shown by the fact that the related system $1T$-TaS_2 has long been understood as a Mott insulator [14]: it is then fully conceivable that Mottness also plays important roles in other TMD. From this viewpoint, much as in the more recent examples of intense interest, melting of the excitonic CDW order in a PEL scenario would necessarily enhance excitonic fluctuations, which could act as an unconventional electronic "pairing glue" for emergence of the competing SC order. However, the theoretical situation still remains unclear, and FS nesting as well as strong electron-phonon views are still claimed to be the instigators of CDW order and SC in pressurized or doped systems [12].

The well-studied $1T$-$TiSe_2$, one of the two polytypes ($1T$, $2H$) in the TMD family where the triangles of chalcogen atoms are oppositely oriented above and below the transition-metal ion (in a distorted CdI_2 structure, see Wypych *et al.* [15]) is a particularly relevant case in point. Careful experimental work has unraveled behavior that consistently fails to fit into any conventional views. We list the problems here:

(i) While optical studies [16] show that the normal to CDW transition is a semimetal to semiconductor transition

*arghya@phy.iitkgp.ernet.in

a la the Overhauser scenario, noticeable spectral weight transfer (SWT) over an energy scale of order 1.0 eV upon heating from 10 to 300 K, along with an almost isosbestic point as a function of temperature below $T_{\rm CDW} \sim 200$ K and a large normal-state scattering rate support sizable electronic correlations.

(ii) Pure $1T$-$TiSe_2$ shows bad-metal resistivity, much above the Mott limit, even at pretty low $T(\ll T_{\rm CDW})$, with a maximum, but no anomaly, in $d\rho/dT$ at $T \simeq T_{\rm CDW}$ [17]. Tellingly, recovery of good metallicity at high pressures also destroys SC. Such a correlation is repeatedly seen in many systems where unconventional SC appears near Mott insulators and magnetism [18] (however, TMD never show magnetism, nor has Mottness been hitherto considered important, except for $1T$-TaS_2 [14] and $2H$-$TaSe_2$ [9,13]). This suggests that strong normal-state scattering also facilitates SC pair formation below T_c.

(iii) ARPES data [19] show that the renormalized electronic structure in the normal state ($T > T_{\rm CDW}$) already resembles a local density approximation (LDA) dispersion modified by excitonic correlations, supporting a PEL view. Moreover, lack of clear polaron effects (e.g, kinks in the band dispersion at phonon energies, well below E_F in resonant inelastic x-ray scattering [10]) and, more importantly, the insensitivity of ARPES band dispersions to atomic displacements occurring across $T_{\rm CDW}$, argue against a band JT instability, even though electron-lattice coupling is ubiquitous to TMD [20].

(iv) Finally, in spite of the incoherent metal features pointed out above, the effective mass is only weakly renormalized above $T_{\rm CDW}$.

These observations put strong constraints on an acceptable theory. Most importantly, they conflict with both FS nesting and band JT views on general grounds: Absence of band quasiparticles in the normal state rules out a conventional ordering instability involving the LDA Fermi surface (FS) features. Simply put, the very concept of a well-defined FS in the LDA sense becomes untenable in bad metals. As pointed out above, ARPES data also argue against a band JT instability to CDW order. Weak mass renormalization above $T_{\rm CDW}$ conflicts with one-band modeling, but not with a multiband approach [21]: even in the classic Mott case of V_2O_3, the effective mass in the correlated metal is only moderately enhanced near the (undoubtedly correlation-driven) metal-insulator transition [21,22]. Thus, taken together, these observations force one to view emergence of the CDW as a strong coupling Overhauser instability of a multiband bad-metal normal state without LFL quasiparticles.

These issues have been selectively addressed earlier within conflicting theoretical views, but the above observations force us to critically reexamine them. Here, we show that these anomalous responses are naturally understood within our PEL view [9] for $1T$-$TiSe_2$, strongly supporting the PEL as a novel (and perhaps generic) alternative to conventional theories for TMD. In remarkable parallels with d and f band systems close to Mottness and unconventional order(s), we unravel a new instance of a selective metallic state in the PEL, and construct a scenario for the instability of this PEL to a low-T CDW state. Our philosophy is opposite in spirit to weak coupling Fermi liquid ones, and is actually closer to resonating valence bond (RVB) ideas [23], in the sense that ordered state(s) arise as two-particle (BEC) instabilities of an incoherent liquid of preformed excitons.

II. METHOD

LCAO band structure for $1T$-$TiSe_2$ was constructed [24,25] by using the Ti d and Se p states. This gives two bands closest to E_F (predominantly Ti d_{xy} and Se p_z) [Figs. 1(a) and 1(c)] as well as the FS [Fig. 1(b)] in very good accord with earlier results [24,25], as shown in Fig. 1. A sizable d_{xy}-p_z mixing hybridizes the small number of electrons and holes. In this situation, even moderate electronic correlations

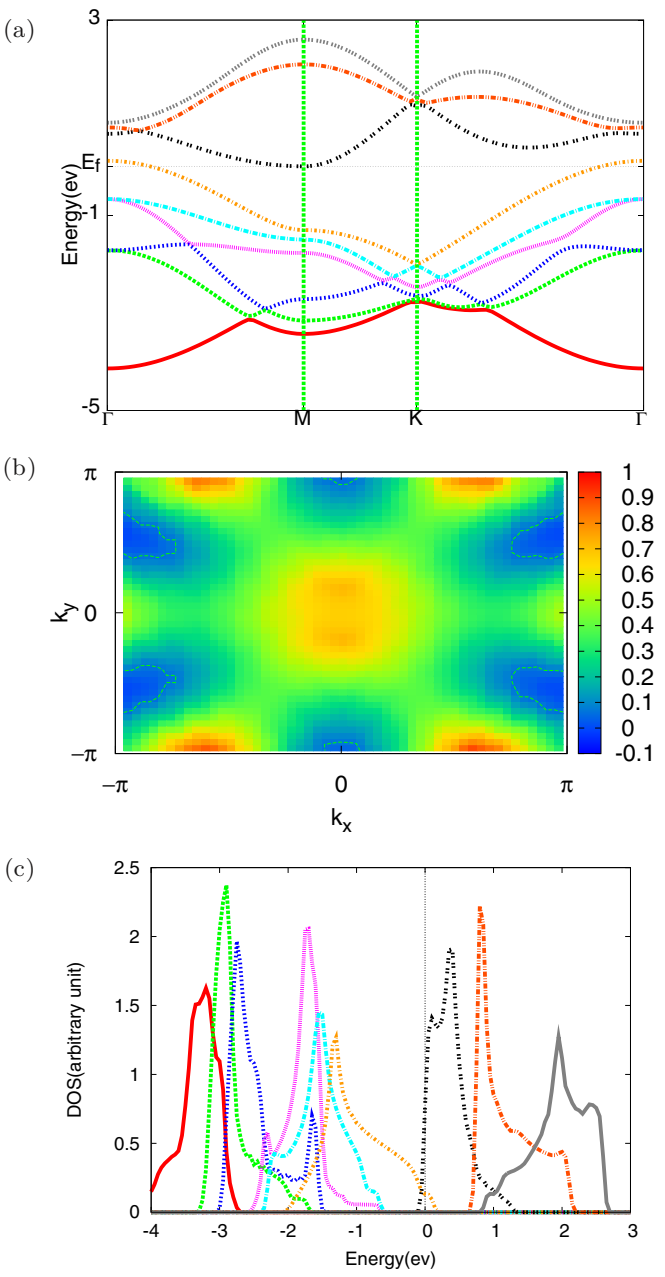

FIG. 1. (Color online) (a) Tight-binding band structure, (b) Fermi surface map, and (c) density of states plot for the Ti d t_{2g} and Se p bands. The multiorbital DMFT involves the two bands, Ti d (black) and Se p (yellow), that straddle the Fermi level.

(<1.0 eV) facilitate exciton formation already at high T, as already discussed by Halperin *et al.* [5] in the 1960s. Given that electronically active states comprise d_{xy} and p_z band states, an intraband Hubbard $U \simeq 1.0$ eV and interband correlation $U_{ab} \simeq 0.5$–0.7 eV are realistic values: these can be estimated from a first-principles, constrained LDA calculation, and we believe [26] that these fall in the range quoted above.

Although static Hartree-Fock (HF) theory can now give a CDW *ground*-state [11,19] description of observed normal-state incoherence, and in general, preformed liquidlike electronic states, lies outside its scope. Thus, the character and ordering instabilities of such bad metals *cannot*, by construction, be rationalized by appealing to static mean field theory: this can only be reliably accessed by approaches which can adequately capture dynamical correlations. For $1T$-$TiSe_2$, a minimal two-band Hubbard model as defined below is mandated by LCAO results, and adequate treatment of dynamical correlations underlying incoherent behavior is achieved by dynamical mean field theory (DMFT). DMFT and cluster DMFT approaches have, by now, a proven record of successfully treating strong dynamical fluctuations in correlated electronic systems, making them preferred tools of choice in the present context. The two-band Hubbard model we use is (calling $d_{xy} = a$ and $p_z = b$)

$$H_{el} = \sum_{\mathbf{k},l,m,\sigma} \left(t_{\mathbf{k}}^{lm} + \epsilon_l \delta_{lm}\right) c_{\mathbf{k}l\sigma}^{\dagger} c_{\mathbf{k}m\sigma} + U \sum_{i,l=a,b} n_{il\uparrow} n_{il\downarrow} + U_{ab} \sum_{i} n_{ia} n_{ib},$$

where l,m run over both band indices a,b, the intraorbital correlation is U (taken to be same for a, b bands, we have checked that results are insensitive to this choice within reasonable limits), U_{ab} is the interorbital correlation term that, along with $t_{\mathbf{k}}^{ab}$, will play a major role throughout. Further, in TMD, the most relevant A_{1g} phonon mode couples to the interband excitons [11] by symmetry, and the electron-phonon coupling is $H_{el\text{-}l} = g \sum_i (A_i + A_i^{\dagger})(c_{ia}^{\dagger} c_{ib} + \text{H.c.})$. (We have taken $g = 0.05$ after checking all possible realistic values to get a good description of experiments.) To solve $H = H_{el} + H_{el\text{-}l}$ within DMFT, we have combined the multiorbital iterated perturbation theory (MOIPT) for H_{el} [21] with the DMFT for polarons by Ciuchi *et al.* [27,28] (see Appendix). Actually, this involves extending the polaron-DMFT to multiband cases, seen by writing $H_{el\text{-}l} = g \sum_i (A_i + A_i^{\dagger})(n_{i,+} - n_{i,-})$ by a rotation; $c_{i,\pm} = (c_{i,a} \pm c_{i,b})/\sqrt{2}$ and $n_{i,\pm} = c_{i,\pm}^{\dagger} c_{i,\pm}$. Finally, we extend the normal-state DMFT to the broken-symmetry CDW phase [9]. This is justified since, from the above discussion and LCAO+DMFT results below, we find, *a posteriori*, an incoherent PEL. Instability to CDW order then cannot occur via the traditional band folding of well-defined Fermi liquid (FL) quasiparticles. Rather, as coherent one-particle interband mixing is inoperative, ordered states must now arise directly as two-particle instabilities of the bad metal. For $1T$-$TiSe_2$, the residual two-particle interaction, obtained to second order is proportional to t_{ab}^2, more relevant than the (incoherent) one-electron mixing t_{ab}. The interaction $H_{\text{res}} \simeq -t_{ab}^2 \chi_{ab}(0,0) \sum_{\langle i,j\rangle,\sigma\sigma'} c_{ia\sigma}^{\dagger} c_{jb\sigma} c_{jb\sigma'}^{\dagger} c_{ia\sigma}$, with χ_{ab} the dressed interorbital susceptibility estimated from the normal-state DMFT results. Starting with the new Hamiltonian $H = H_n + H_{\text{res}}^{\text{HF}}$, where $H_n = \sum_{k,\nu} (\epsilon_{k,\nu} + \Sigma_\nu - E_\nu) c_{k,\nu}^{\dagger} c_{k,\nu} + \sum_{a \neq b,(k)} t_{ab} (c_{k,a}^{\dagger} c_{k,b} + \text{H.c.})$, with $\nu = a,b$ and $H_{\text{res}}^{\text{HF}}$ is found by decoupling the intersite interaction in a generalized HF sense. This yields two competing instabilities: $H_{\text{res}}^{(\text{HF})} = -\sum_{\langle i,j\rangle,\sigma\sigma'} (\Delta_{1b} c_{ia\sigma}^{\dagger} c_{ia\sigma} + \Delta_{ab} c_{ia\sigma}^{\dagger} c_{jb-\sigma}^{\dagger} + a \to b)$, with $\Delta_{\text{CDW}} = (\Delta_{1a} - \Delta_{1b}) \propto \langle n_a - n_b \rangle$ representing a CDW and $\Delta_{ab} \propto \langle c_{ia\sigma} c_{jb-\sigma} \rangle$ a multiband spin-singlet SC. Following earlier procedure [9], we compute DMFT spectral functions and transport properties in the CDW state at low T, leaving SC for the future.

A few remarks about our strategy to derive the CDW ordered state and physical observables therein are in order. Our approach to CDW order is very different from that employed in traditional calculations, where the order parameter is self-consistently computed from the off-diagonal element of the matrix Green's function in presence of an infinitesimal symmetry-breaking field. Such a route can be readily adapted to the DMFT calculations. But, in the absence of coherent quasiparticles, such a description of ordered states presents a problem. Since the normal state is an incoherent metal (the associated Green's functions have branch cut structure instead of a renormalized pole structure in the infrared), higher-order multiparticle processes discussed above are inherently involved in the ordering instability. This immediately poses a problem for a traditional BCS-Eliashberg approach, which is valid as long as the bosonic "glue function" is a smooth analytic function of energy. Another way of arguing this point is to notice that the conventional route to a BCS-type instability crucially relies on the fact that the noninteracting FS, though quantitatively modified by interactions, preserves its adiabatic continuity to the noninteracting FS. As soon as this continuity is lost at selective Mott instabilities, where parts of the LDA (or LCAO in our case) FS are eaten up by band selective correlations, a BCS-type instability becomes untenable. Our approach above is analogous to the one used for coupled $D = 1$ Luttinger liquids, where derivation of ordered states by studying the most relevant two-particle instabilities is a well-known and tested procedure in coupled one-dimensional systems such as organics [29]. In our local approximation, the only difference, following from our finding of a local non-FL state, is the replacement of coupled $D = 1$ chains by coupled $D = 0$ "impurities," and, as mentioned above (see also earlier work [9]), H_{res} is the most relevant interaction when coherent single-particle tunneling is suppressed in the incoherent metal.

III. RESULTS

We now show how the approach envisaged above gives a very good account of a whole range of physical responses. The DMFT spectral function without electron phonon coupling is shown in Fig. 2. We observe that the density of states for either band is weakly temperature dependent in the normal state, but starts developing pseudogap features at lower T as CDW order sets in. Turning on the electron-phonon coupling has a more dramatic effect. Even at $g = 0.05$, a CDW ground state is obtained, and the one-particle spectral functions begin to display different features as compared to the $g = 0$ case, as discussed in the following.

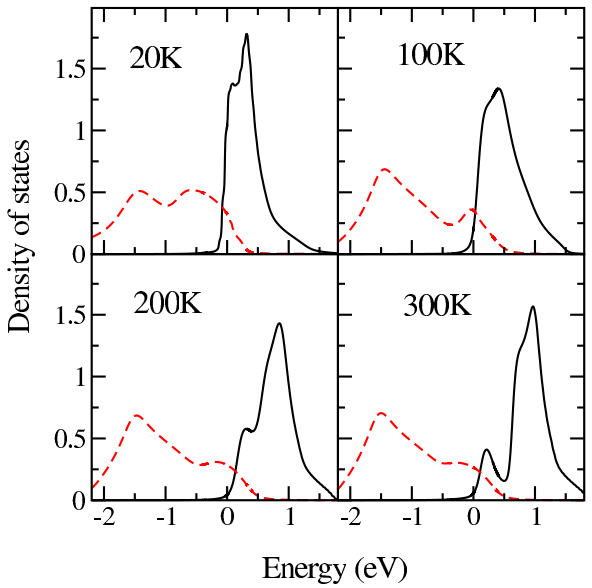

FIG. 2. (Color online) Spectral function from DMFT calculations at different temperatures (20–300 K) without phonon coupling ($g = 0$).

We show the DMFT many-body spectral function for the Ti d and Se p bands in Fig. 3(a) and the corresponding self-energies in Figs. 3(b) and 4(a) and 4(b), at both high ($T > T_{\rm CDW}$) and low ($T < T_{\rm CDW}$) temperatures. ($T_{\rm CDW}$ can be identified by several means in our theory: it is the scale at which the pseudogap feature first appears in the DOS. It is also the scale where the resistivity starts to become coherent. Considering these criteria, we estimate that $T_{\rm CDW} \simeq 170$ K.)

The spectral function shows clear "semimetal" features, which, however, are not those of a conventional semimetal in the sense of an uncorrelated one-electron band-structure view. A sharp "polelike" feature is seen at lower temperatures exactly at the Fermi level in both (a and b band) spectral functions (Fig. 3(a)), and a gap is seen above E_F. This sharp feature is a result of coupling of an orbital-selective metal to phonons, as argued below. As temperature increases beyond about 150 K, this sharp feature vanishes. The density of states at the Fermi level develops an incoherent pseudogap feature at low energies.

Interestingly, examination of the self-energies bares the hidden selective Mottness in the system. In Fig. 3(b), the imaginary part of the $T = 0$ self-energies is shown. It is clearly seen that at $\omega = 0$, a pole exists in $\mathrm{Im}\Sigma_b(\omega)$, signaling Mott localized b states, while the a band states exhibit incoherent Fermi liquid ($-C_1 - C_2\omega^2$) behavior. This orbital selectivity is responsible for a wide range of anomalies, e.g, bad-metallic normal-state resistivity, as argued in the following. Further, the temperature evolution of spectral features, shown in Fig. 4(a), reveals the connection to the CDW instability. The panels on the left correspond to the Ti d band self-energy while those on the right are for the Se p band. The temperature dependence of the Ti d band self-energy has an incoherent Fermi liquid form, i.e., $-(c + a\omega^2 + bT^2)$. The Mott pole in $\mathrm{Im}\Sigma_b(\omega = 0)$ shows hardly any changes until $T \sim T_{\rm CDW}$, when it is replaced by a gap structure. This signals onset of enhanced

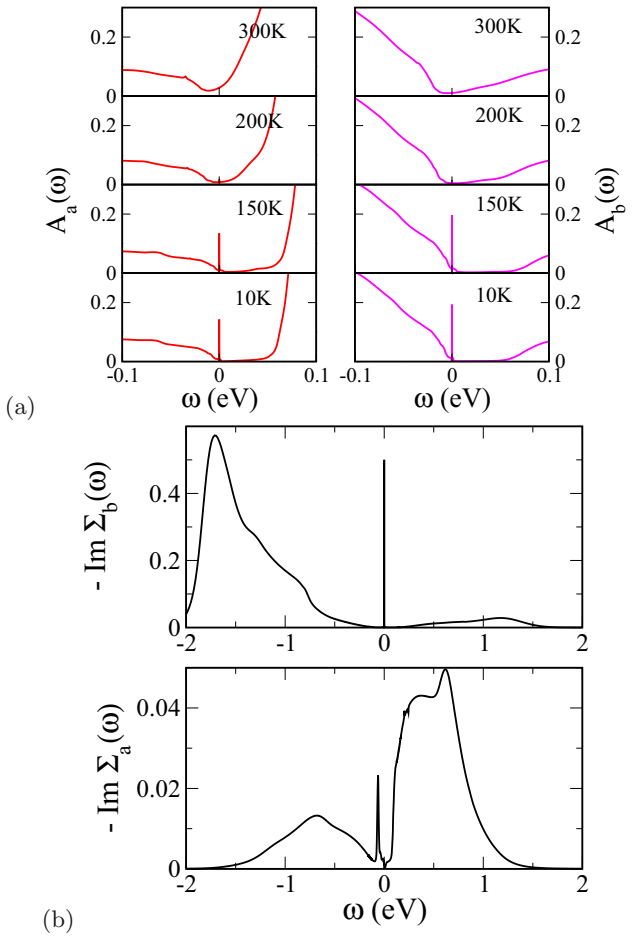

FIG. 3. (Color online) (a) Temperature evolution of spectral function of a (Ti d: left panel) and b (Se p: right panel) bands; (b) the imaginary part of the self-energies at $T = 0$.

orbital selectivity below $T_{\rm CDW}$, and the reason for emergence of the sharp peak in the local spectral functions at $\Omega \simeq -0.07$ eV is that sizable reduction of strong "normal"-state incoherence upon CDW gap stabilization sharpens up the low-energy feature that exists due to electron-phonon coupling (but which is washed out by strong scattering above $T_{\rm CDW}$).

Thus, existence of orbital selectivity (OS), found already in the normal state, is now related to strong normal-state scattering, rather than the onset of CDW order (which, however, further enhances it). Finding of OS in $1T$-$TiSe_2$ is surprising (Ti being nominally d^0), but can be traced back to the fact that, in presence of a small number of electrons and holes induced by t_{ab}, even a moderate U_{ab} leads to exciton formation, and hence to selective Mottness in the multiband situation that obtains in $1T$-$TiSe_2$. Since $\Delta_c = (\epsilon_b - \epsilon_a)$ is already finite at LCAO level, this results in an intrinsic orbital selectivity when correlations are swithced on [30]. The microscopic reason is that local intraorbital and interorbital correlations renormalize this "crystal-field" term already at the Hartree level (while the dynamical contributions to the self-energies quantify the *changes* in dynamical spectral weight transfer in response to changes in Δ_c). This trend is enhanced upon emergence of exciton-driven CDW order since gap formation

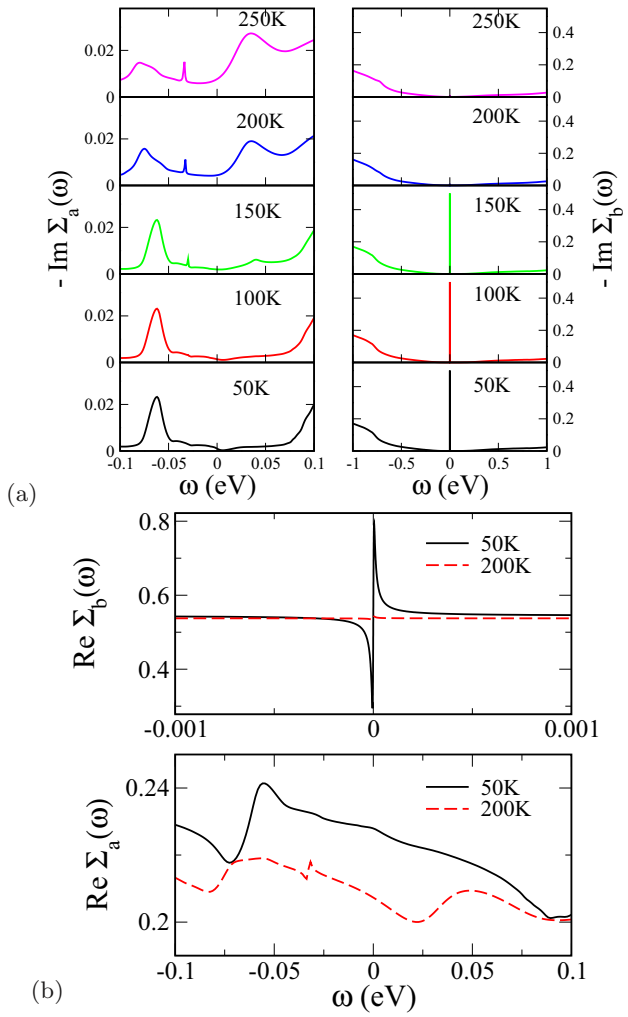

FIG. 4. (Color online) (a) Temperature dependence of the imaginary part of the self-energy close to the Fermi level. (b) Real part of the self-energy for Ti d and Se p bands at $T = 50$ K ($<T_{\rm CDW}$) and $T = 200$ K ($>T_{\rm CDW}$).

involving interband excitons further renormalizes it. Recall that the original idea of Mott was in fact indelibly tied to quantum melting of correlation-induced excitons under pressure. Intriguingly, in $1T$-$TiSe_2$, stabilization of excitonic CDW order enhances selective Mott features at lower T, as emergence of the $\omega = 0$ pole in $\mathrm{Im}\Sigma_b(\omega)$ clearly shows. Simultaneously, however, examination of $\mathrm{Re}\Sigma_a(\omega)$ also clearly shows small mass enhancements, which must now arise solely from the a band carriers. In extant literature [10], this finding below $T_{\rm CDW}$ is proposed as a concrete example of a *reduced* effective mass due to renormalization effects caused by the appearance of a strong periodic potential below $T_{\rm CDW}$. Our results are certainly in accord with this finding. As mentioned before, no large mass enhancements are theoretically (at least within DMFT) expected in a multiband system, even in an orbital-selective Mott regime. As T is reduced, this feature goes hand-in-hand with slight stabilization of the normal-state gap in the *total* spectral function, now interpreted as a true CDW gap. As advertised before, and in full accord with experimental data, sizable T-driven SWT accompanies the transition.

It is natural to inquire as to the microscopic origins of these changes. Above $T_{\rm CDW}$, the b band states are Mott localized due to exciton formation (however, this is a regime where excitons have not condensed, hence the lack of a clean CDW gap in the spectra). Below $T_{\rm CDW}$, appearance of CDW order via our mechanism modifies the high-T features as follows: having excitonic CDW state implies CDW order arising in tandem with a modification of excitonic correlations (from incoherent to coherent below $T_{\rm CDW}$). Mathematically, within our formulation, this translates into an effective modification of the interband excitonic average $\langle a^\dagger_{i\sigma} b_{i\sigma}\rangle = -(1/\pi)\int \mathrm{Im}G_{ab}(\omega)d\omega$. Examining the structure of the effective residual interaction above, this change arises from the Hartree-Fock decoupled form of $H^{(2)}_{\rm res}$ in the interband spin-singlet particle-hole sector. Its form implies an additional, interband a-b mixing and will generically give rise to more consequences: (i) Opening of a CDW gap, increasing low-energy coherence, but now due to broken symmetry and not due to FL effects, and (ii) cutting off the divergence implied by selective Mottness by reappearance of the b-fermion recoil, now due to $H^{(2)}_{\rm res}$. We emphasize that this should not be confused with b-fermion recoil giving rise to a correlated FL metal in DMFT: in principle, this can also happen. But, while the latter leads to a direct cross over from an incoherent to a FL metal at low T, the former leads to a direct transition from an incoherent metal to an ordered state. In this context, the low-energy peak in $\rho_{a,b}(\omega)$ below $T_{\rm CDW}$ is due to sharpening of the phonon spectral function once CDW order sets in, and has nothing to do with FL effects. This is around $(-)0.07$ eV, in the background of the CDW gap. That this interpretation is consistent is shown by the observation that this structure vanishes for $T > T_{\rm CDW}$, when the strong normal-state incoherence damps out the coherence associated with having sharp structures.

If the PEL alternative is to be credible, the full range of observations must be explicable without any additional assumptions. In Fig. 5 we compare our DMFT one-particle spectral function $A_{a,b}(\mathbf{k},\omega) = -\mathrm{Im}G_{a,b}(\mathbf{k},\omega)/\pi$, and renormalized band dispersion $E_{\mathbf{k},a} = \epsilon_{\mathbf{k},a} + \mathrm{Re}\Sigma_{\mathbf{k},a}(\epsilon)$, with ARPES data [19] where these exist. This is already a stringent test for theory: while LDA plus static HF can conceivably yield agreement with band *dispersions*, the real test is a simultaneous description of the ARPES line shapes. For a dynamically fluctuating "liquid," the latter is expected to show broad continuumlike features without infrared (LFL quasiparticle) poles. Rather remarkably, our LCAO+DMFT results provide a nice semiquantitative description of extant ARPES dispersions and line shapes up to rather high energies. In particular, they bare the preformed excitonic features in $E_{\mathbf{k},a,b}$ and clear, associated "gap" features in ARPES line shapes above $T_{\rm CDW}$. Very good accord in all details, including the band positions, their intensity distributions, and band shifts as a function of T, with the ARPES dispersion is clear from a direct comparison between our Fig. 6 with Fig. 2 of Monney *et al.* [19]. In particular, we can even identify the detailed features in the T dependence of the ARPES intensity (Fig. 6) with data: (i) the peak at $\simeq -0.2$ eV is identified as the valence band backfolded to the M point by comparing the red curve in Fig. 6 with the top panel in Fig. 5. (ii) A new peak, labeled C by Monney *et al.*, also appears below $T_{\rm CDW}$ and gets more pronounced upon decreasing T, precisely as seen. (iii) The

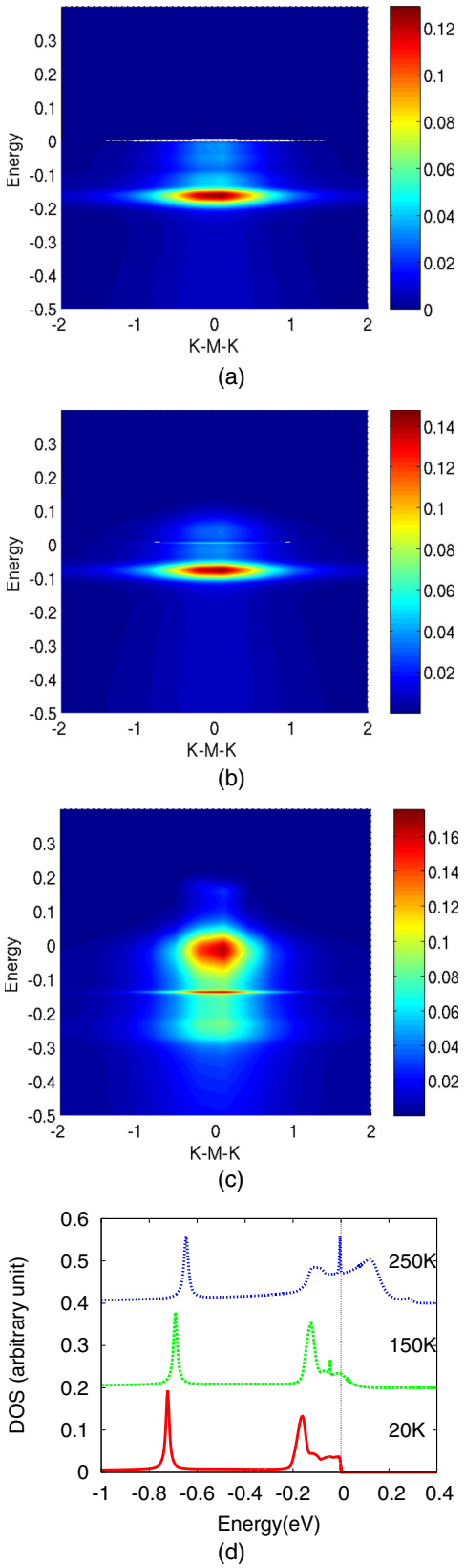

FIG. 5. (Color online) Theoretical ARPES map along K-M-K direction of the Brilluoin zone at (a) 20 K, (b) 150 K, and (c) 270 K. (d) EDC at M point at the temperatures shown.

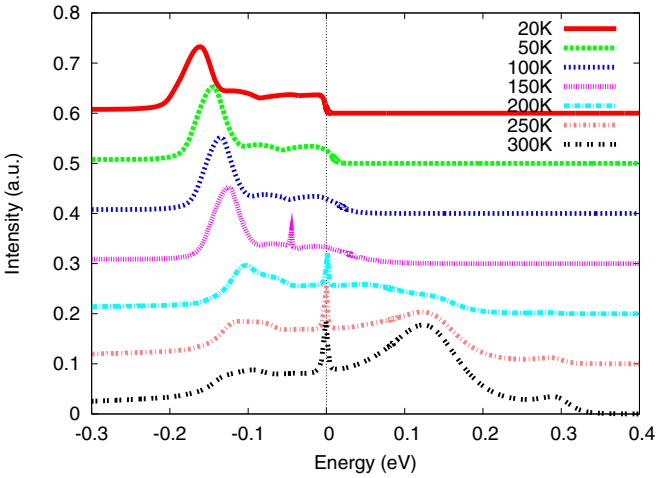

FIG. 6. (Color online) Theoretical ARPES spectra at M point at different temperatures. As temperature increases across $T_{\rm CDW}$, the peak in the DMFT spectral function crosses the renormalized Fermi energy (E_F).

peak D, identified as a "quasiparticle peak" originating from coupling to phonons in experiment is also obtained in DMFT in very good qualitative accord with data: especially interesting is that it is quickly damped out as T increases, exactly as seen in the top four curves in our Fig. 6. However, at high T, we resolve an additional (sharper) low-energy peak, also arising from electron-phonon coupling, which remains dispersionless above $T_{\rm CDW}$: this feature is not seen in the ARPES results of Monney *et al.* Finally, we also cannot observe peak A, identified with a second, spin-orbit split, valence band since we have not used the full set of Se p and Ti d bands in this work. Nevertheless, the accord between theory and experiment is quite good with regard to features relevant for the CDW in $1T$-$TiSe_2$.

We now consider the ARPES band-structure maps. At high T, along K-M-K direction in the Brillouin zone the putative valence band (VB) heavily damped by strong (due to preformed excitons) scattering crosses $E_F(=0)$ while the putative conduction band (CB) lies totally above E_F. This conflicts with the LDA [or LCAO, see Fig. 1(a)] results, which predict a sizable overlap between VB and CB states at E_F, and reflects the failure of the FS nesting mechanism in the *real* one-particle spectra. (In fact, to cure such conflicts, the standard explanation within conventional views has been to attribute such discrepancies between LDA and ARPES data to uncontrolled excess [10] of Ti. Our view naturally produces this, without having to take recourse to such extraneous conditions.) Clear Hubbard band shakeup features in DMFT are also seen in the color plot: in particular, we predict that the $\omega > 0$ part of the line shape (at M point in Fig. 6) should lend itself to observation in inverse ARPES (ARIPES) studies in the future. In addition, comparison of the DMFT energy distribution curve (EDC) with extant ARPES results at the M point also shows very good accord as a function of T over the whole range. A moderate band narrowing of LCAO bands and broad spectral line shapes with appreciable T-dependent SWT in one single system are generic fingerprints of strong dynamical correlations in multiorbital systems and so, as

alluded to before, the second feature above, essential for describing liquid correlations, cannot be accounted for by a static HF theory, as done so far [11].

Detailed Fermi surface (FS) maps as a function of T in $1T$-$TiSe_2$ are rare. We have taken the FS mapped out by Rossnagel *et al.* [31] to study how the PEL idea survives this important test. While instabilities driven by LDA FS form the backbone of weak coupling or itinerant views, it is also possible, in a renormalized itinerant or Mottness-based theories, that these could involve a *new* FS sizably reconstructed by correlations. That the FS does not reconstruct across T_{CDW} in $1T$-$TiSe_2$ was one of the main (among others, see above) arguments for invoking unconventional PEL scenarios in the first place. Close inspection of FS evolution across T_{CDW} shows that, while this is undoubtedly correct, there are still specific features which any theory needs to confront: (i) the band pockets are smeared out at high temperature ($T > T_{CDW}$) and, more importantly, a much brighter ring structure appears at the M point below T_{CDW}.

In Fig. 7, we show our DMFT FS from low (top panel) to high T (bottom panel). As expected due to strong PEL scattering, the high-T FS is sizably smeared out [arises from the finite $\mathrm{Im}\Sigma_a(\omega = 0)$ at 200 K from Fig. 4(a)]. Remarkably enough, we *also* find a clear ring feature at the M point below 150 K (upper panel), in remarkable accord with data. Since this ringlike feature becomes well defined only below T_{CDW}, it is a direct consequence of CDW order-induced reconstruction of electronic states. This is fully consistent with the excitonic CDW view, where CDW follows excitonic "solid" order, and the latter arises principally via interplay between $t_{ab}^{\mathbf{k}}$ and U_{ab}, implying backfolding of Se p band from the Γ point due to the $2 \times 2 \times 2$ CDW superstructure formation. Further, close observation of DMFT results shows that the central pocket around the Γ point has seemingly developed elongated shape instead of the hexagonal shape expected from the LCAO result. We believe that this important modification, hitherto not noted sufficiently, arises due to an orbital-dependent electronic-structure reconstruction that is essentially driven by the $\mathbf{k}$-dependent form factor of the interorbital hybridization [$t_{ab}(\mathbf{k})$]. Experimental confirmation of this feature would thus constitute additional support for a PEL scenario. Finally, the stabilization and slight increase of the normal-state "gap" below T_{CDW} also accords with optical data [16] and with the semimetal-to-semiconductor characterization of the normal-CDW transition in $1T$-$TiSe_2$.

Thus, such quantitative agreement between our excitonic DMFT results premised upon a novel PEL view and ARPES in all important details lends strong credence to the idea of a dynamically fluctuating excitonic liquid at high T giving way to a low-T CDW order. However, to further qualify as a credible candidate, the *same* formulation must also describe transport as well. Fortunately, in DMFT, this task is simplified: it is an excellent approximation to compute transport coefficients directly from the DMFT propagators $G_{a,b}(k,\omega)$ [32] since (irreducible) vertex corrections rigorously vanish for one-band models, and turn out to be surprisingly small even for the multiband case.

In Fig. 8, we show the optical conductivity $\sigma(\omega)$ as a function of T, wherein very good accord with data up to an energy $\simeq O(0.8)$ eV is clear. A clean CDW gap at low T closes

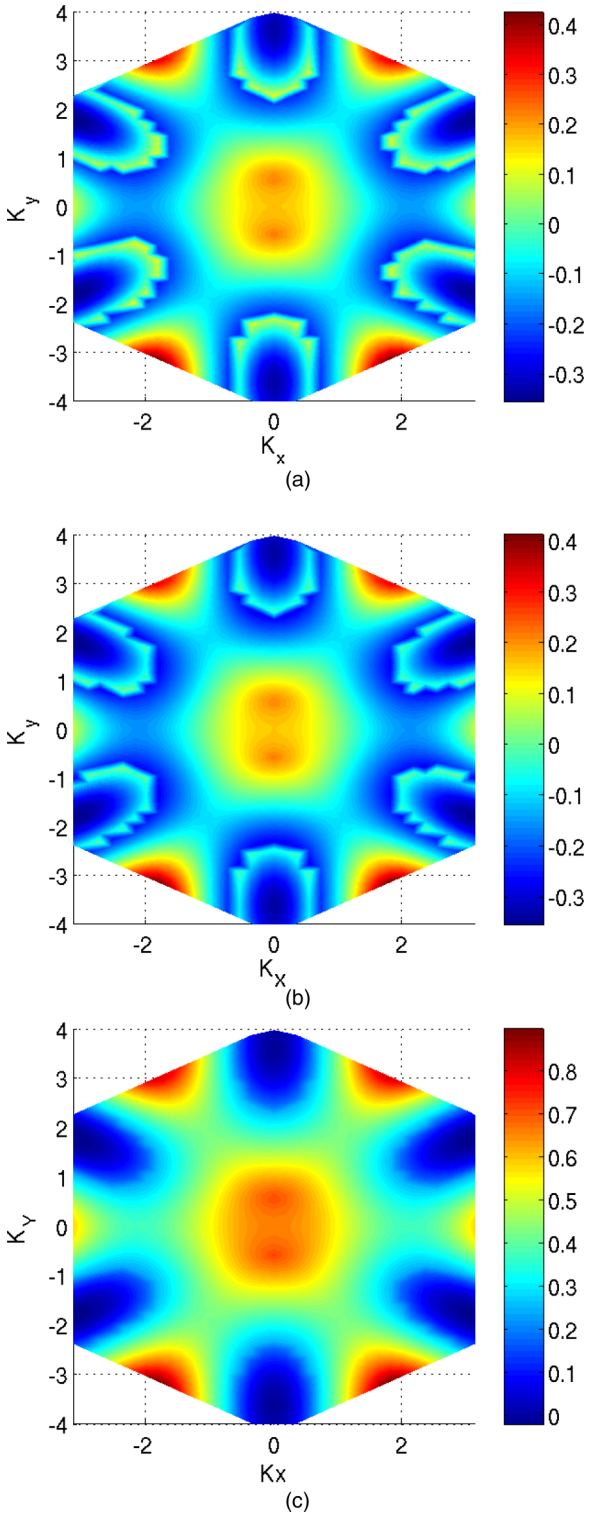

FIG. 7. (Color online) DMFT Fermi surface map at (a) 20 K, (b) 150 K, and (c) 270 K, showing good agreement with the temperature evolution of the Fermi surface in ARPES data of Rossnagel *et al.* [31].

rapidly with increasing T via rapid spectral weight transfer from the relatively sharply defined hump at 0.4 eV to the infrared regions, precisely as seen. Given that we have kept only the two bands crossing E_F in LCAO, agreement at higher

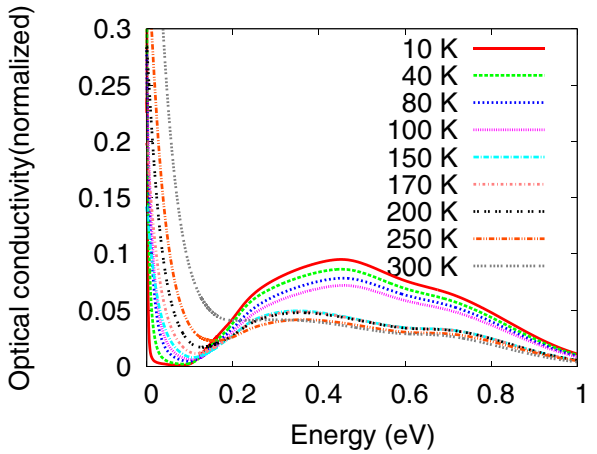

FIG. 8. (Color online) DMFT results for optical conductivity at various temperatures across $T_{\rm CDW}$.

energy ($\gtrsim$0.8 eV) is not expected. The relative sharpness of the low-energy optical response at low T is deceptive: it is not a FL Drude peak, and in fact (fully consistent with the selective Mott behavior in the DMFT spectra above) no FL coherence sets in, even at lowest (10 K) T in DMFT. It is rather a reflection of reduced incoherence due to CDW gap opening. Finally, we also resolve a near isosbectic point in $\sigma(\omega,T)$ curves [where $\sigma(0.2\ \text{eV})$ remains invariant] at different T: this is clear manifestation of sizable dynamical correlations [9], and is again in good accord with the isosbectic point seen around 0.27 eV in the optical study [16].

The DMFT resistivity (Fig. 9) also shows an insulatorlike behavior above $T_{\rm CDW}$, a broad peak without any anomaly below $T_{\rm CDW}$, and bad-metallic behavior below $T_{\rm CDW}$, in full accord with data [17]. The insulatorlike behavior for $T > T_{\rm CDW}$ is a reflection of the large normal-state incoherence, hence carriers strongly scatter off fluctuating, incoherent (preformed) excitons. The bad-metallic behavior below $T_{\rm CDW}$ is then naturally

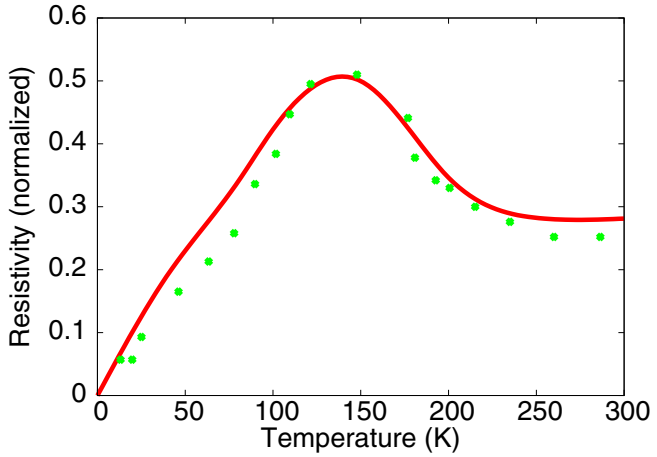

FIG. 9. (Color online) Temperature-dependent dc resistivity within DMFT. Except for the low-T part, LCAO+DMFT results agree very well with experimental results (represented by points, after Li *et al.* [16]), including a broad maximum, rather than a sharp nonanalytic change, across $T_{\rm CDW}$ (see text).

attributable to reduction of this strong normal-state scattering due to (i) opening up of a CDW gap, and (ii) concomitant increase in the tendency to excitonic coherence. Given the bad-metallic resistivity, the consequent short scattering mean-free path [in fact, $k_F l \simeq O(1)$] invalidates a quasiclassical Boltzmann equation-based approach to transport. Interestingly, this is precisely the regime where DMFT should work best. The absence of a sharp ordering anomaly at $T_{\rm CDW}$ is additional evidence against a weak coupling view of the instability. In fact, in a weak coupling instability, resistivity should have shown a sharp ordering anomaly at $T_{\rm CDW}$ on general grounds [33] (in addition, $d\rho/dT$ must also show critical behavior, with exponents linked to those extracted from thermodynamic measurements). The strong coupling view is further supported by finding of a large $2\Delta/k_B T_{\rm CDW} \simeq 7$–10 in TMD (about 7 for $1T$-$TiSe_2$ and 10 for $2H$-$TaSe_2$ [34]). This feature is reminiscent of high-T_c cuprates [35] and implies that CDW formation is associated with a BEC, rather than a BCS-type scenario for the exciton instability. Also, strong inelastic scattering needed to rationalize bad metallicity above $T_{\rm CDW}$ and sizable T-induced SWT are characteristic signatures of a strong coupling limit.

Thus, taken together, very good accord with ARPES and transport data strongly supports our basic hypothesis: (i) the normal state is a strongly fluctuating liquid of incoherent excitons, and (ii) CDW order in $1T$-$TiSe_2$ must fall into the strong coupling class, qualitatively different from a conventional Overhauser transition of well-defined band (LFL) quasiparticles.

Emergence of CDW order from a PEL should leave further specific signatures in other data. First, CDW and excitonic correlations must now track each other beyond $T_{\rm CDW}$, well into the PEL state. In Fig. 10, we show the excitonic and CDW order parameters $\Delta_{\rm exc} \propto \langle \Gamma^x \rangle = \langle (c^\dagger_{ia} c_{ib} + \text{H.c.}) \rangle, \Delta_{\rm CDW} \propto \langle \Gamma^z \rangle = \langle n_a - n_b \rangle/2$, along with their T derivatives, as a function of temperature (T). In particular, as expected in the PEL scenario, *both* follow each other and are finite way above $T_{\rm CDW}$ in nice qualitative accord with the T dependence of the CDW order parameter from ARPES [19]. In fact, a simple estimate of the change of the value of the order parameter can be made by plugging in the value of U_{ab} in our Fig. 10 to compare with Fig. 12(d) of Monney *et al.* [36]. The resulting change (about 35 meV) from high to low temperature is reproduced correctly. The absence of a conventional (BCS-type) mean field transition can be rationalized by noticing that, in presence of the elelctron-lattice coupling $H_{el\text{-}l} = g \sum_i (A_i + A_i^\dagger)(c^\dagger_{ia} c_{ib} + \text{H.c.})$, the universality class of the normal-CDW transition turns out to be that of an Ising model in an external field. This implies that the (mean field) transition is smeared into a smooth crossover. It is indeed true that there is no critical point in the Ising model at a finite field. While this would seem to preempt usage of the order parameter employed, it is the symmetry-adapted coupling to the $(A1g)$ phonons that gives rise to the field that is conjugate to the order parameter. Perhaps what could act as an Ising-type order parameter for this CDW transition is the magnitude of the periodic lattice distortion that the excitonic CDW state must induce. This has recently been worked out (Fig. 3 of Monney *et al.* [37]) in an idealized tight-binding cum static Hartree-Fock approach to

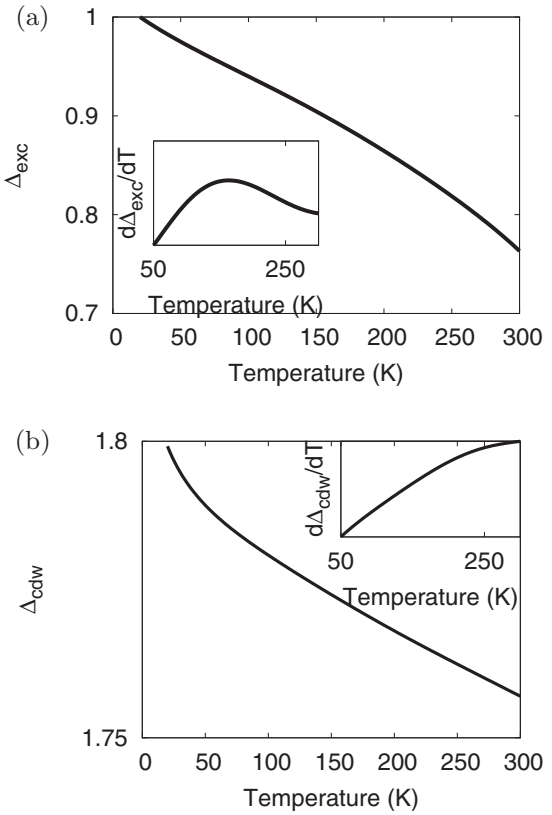

FIG. 10. (a) The interorbital excitonic order parameter [ImG_{ab}, normalized by $\Delta(10)$ K] and its derivative (inset), and (b) the CDW order parameter n_a-n_b ($\propto\Delta_{\rm CDW}$) and its derivative (inset) as a function of T.

the problem, and shows the required features associated with Ising criticality.

All this is related to the difficulty posed by having an unusually smooth variation of the order parameter across $T_{\rm CDW}$ in this system: in fact, one can see a deviation from the high-T value only upon drawing a tangent to the high-T curve (which starts deviating from linearity around 160 K, close to $T_{\rm CDW}$). There is support for this observation in Figs. 12(c) and 12(d) of Monney *et al.* [36], where the CDW order parameter was extracted from ARPES measurements. Within error bars, there is seemingly no sharp change across $T_{\rm CDW}$, and, in fact, the high-T value of the order parameter is already very large (similar behavior is transferred to the behavior of the chemical potential as a function of T).

The relevance of excitonic correlations is also visible as follows. We see that $\rho(T)$ closely follows the T dependence of $d\Delta_{\rm exc}/dT$ above (Fig. 10), but does not show any obvious correlation with $d\Delta_{\rm CDW}/dT$: this shows that the anomalous resistivity is caused by carriers scattering off incoherent excitonic (liquidlike) correlations. In our PEL scenario, the change to metallic behavior in $\rho(T)$ is attributable to reduction of the strong scattering when excitons condense at $T_{\rm CDW}$. True CDW order now follows a true BEC of preformed excitons at lower T.

Given the specific form of the electron-phonon coupling, now also interpretable as coupling of interband excitons to A_{1g} phonon mode by symmetry, the lattice is expected, very generally, to react to the T-dependent changes (incoherent at high T, more coherent at lower T) in exciton dynamics. In particular, the DMFT phonon spectral function, computed from $\rho_{ph}(\omega) = (-1/\pi){\rm Im}D(\omega) = (-1/\pi){\rm Im}[2\Omega_0/(\omega^2 - \Omega_0^2 - 2g^2\Omega_0\chi_{ab}(\omega))]$ and shown in Fig. 11, should mirror excitonic CDW correlations.

Several interesting features stand out: (i) $\rho_{ph}(\omega)$ shows maximum intensity with reduced linewidth around $T_m = 150$ K, precisely where the resistivity peaks. (ii) Above $T_{\rm CDW}$, the phonon spectrum is noticeably broader, reflecting coupling to incoherent excitonic liquid modes, and (iii) asymmetry in $\rho_{ph}(\omega)$ *increases* as T is lowered below $T_{\rm CDW}$. This reflects precursors of a Fano-type structure, arising from treatment of $H_{el\text{-}l}$ beyond the adiabatic limit within our DMFT. Onset of excitonic coherence below $T_{\rm CDW}$ reduces strong normal-state scattering, sharpening the phonon spectrum. (iv) Finally, we find that the detailed T dependence of both the A_{1g}-phonon line shape and linewidth matches nicely with the ones extracted from a Raman scattering study [38]. Only below $T_{\rm CDW}$ is there a discord between measured and computed linewidths: it levels off to a constant in experiment, a feature not captured by our present calculation. The reason is that we have not carried out a study of the change in phonon dynamics below $T_{\rm CDW}$. A full study of lattice effects must rest on a more realistic input to the full phonon spectrum of $1T$-$TiSe_2$, a point we leave for future study. Thus, taken together, very good quantitative accord with a whole host of spectral and transport responses for $1T$-$TiSe_2$ *and* a comprehensive qualitative rationalization of structural features in one single theoretical picture constitutes overwhelming support for a novel PEL view. Thus, the central conclusion of our work is as follows: *The CDW instability must now be interpreted as a strong coupling instability of an incoherent PEL normal state, rather than as a weak coupling Fermi surface nesting instability of a good LFL.*

The above findings have important implications for SC arising under pressure. A finite pressure increases a-b band overlap via t_{ab}, leading to a redistribution of electrons and holes, and weakens excitonic CDW order. From Fig. 10(a), this implies enhancement of excitonic fluctuations, also seen by noticing that a fall of $\langle\Gamma_i^z\Gamma_j^z\rangle$ must transfer weight to

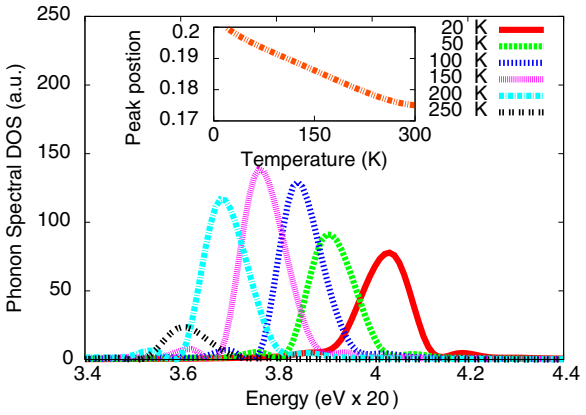

FIG. 11. (Color online) Phonon spectral function at different temperatures. The inset shows change in peak position of the A_{1g} phonon mode with temperature, in good accord with Raman data above $T_{\rm CDW}$ (see text).

the transverse part, i.e., enhance $\langle(\Gamma_i^+\Gamma_j^- + \text{H.c.})\rangle$ via the pseudospin sum rule $\Gamma^2 = \Gamma(\Gamma+1)$. Thus, near the critical $p = p_c$ where CDW is destroyed, we expect a maximization of excitonic fluctuations. These can constitute the critical collective (electronic) fluctuations that could lead to an instability to an interband SC (competing with CDW) with a finite $\Delta_{ab} \simeq \langle c_{ia\sigma} c_{jb-\sigma}\rangle$. However, normal-state incoherence implies that SC must now arise directly from the incoherent metal via a two-particle instability: this can be explored by solving $H = H_{el} + H_{\text{res}}$ in the pair channel. The electron-lattice coupling will further enhance the effective pair interaction in H_{res} above [9]. Even without the benefit of a detailed DMFT calculation for the SC phase, we thus expect the SC T_c to be maximal close to p_c if dynamical excitonic fluctuations mediate Cooper pairing: this is again in accord with observations [17] and the causal link is compelling.

We believe this work also has further important implications on a broader level. Our unexpected finding of OS bad metallicity in the high-T PEL brings $1T$-$TiSe_2$ closer to the bad actors in d and f band systems, where OS is a consequence of orbital-selective Hubbard correlations [39] (or, in the cuprates, momentum-selective correlations [35]). Given that $1T$-TaS_2 has long been known to be a Mott insulator, our proposal of selective Mottness and associated excitonic liquid features is quite reasonable. However, since magnetism is never an issue in the TMDs of interest, what underpins anomalous responses reminiscent of d and f band critical systems near magnetism is moot. The common unifying mechanism seems to be selective Mottness, which is indeed one of the main contenders for understanding anomalous quantum criticality in d and f band systems [40,41]. Selective Mottness itself can always occur via different mechanisms: in particular, depending upon the microscopics of a given system, it can be associated with magnetism, but it clearly does not always need to be so. It can also be associated with other density-wave instabilities in the charge or orbital sectors in multiband systems such as TMDs. Nevertheless, a common element, namely, destruction of Landau FL quasiparticles, would always accompany onset of selective Mottness. Thus, in light of this work, it should not be too surprising that the high-T PEL bears some similarities with the FL* theory [40] in the f electron QCP context. Evidence attesting to this comes from the fact that only the Se p band crosses E_F, while the Ti d band lies above E_F already in the high-T liquid. In other words, the observed FS has already reconstructed from its LDA counterpart to reflect the preformed excitonic character of the normal state. Spectral and transport features show characteristic incoherence features, as expected in an FL* state, and the efficacy of DMFT as a valuable tool to understand these is also known in the f electron context [39,42]. That this identification implies an interesting scenario, similar to those invoked for anomalous metals on the border of $(T = 0)$ magnetism, may also permit a rationalization of the apparent similarities claimed to exist between underdoped cuprates and TMD [12]. Viewed from the perspective of our study, these similarities are, ultimately, manifestations of the selective (bad) metallicity in both cases: momentum selective in underdoped cuprates and orbital selective in $1T$-$TiSe_2$. Thus, we arrive at a perhaps general idea with broader appeal across classes of correlated systems: selective Mottness (whether orbital or momentum) induces critical electronic liquid states characterized by loss of LFL coherence. This collectively fluctuating electronic fluid can subsequently become unstable, either to a myriad (charge, spin, orbital) of density wave orders, or to (competing) unconventional superconductive orders, depending upon the actual microscopics of the system under study. In TMD, material-specific reasons favor competing interband CDW and SC orders from such a strongly fluctuating excitonic liquid.

IV. CONCLUSION

In conclusion, we show that a whole host of physical responses in $1T$-$TiSe_2$, difficult to reconcile with a band FS nesting or band JT mechanisms, provided a natural and good quantitative explication within a new PEL alternative. Finding of orbital-selective Mott features in renormalized normal-state electronic structure via DMFT leads to a very good description of a range of spectral and transport data in both normal and CDW states. More importantly, it brings the TMD closer to the anomalous critical metals of much more recent interest. Along with its success for $2H$-$TaSe_2$ [9], our work relates the PEL idea to a more generic theoretical level for TMD. Particularly interesting should be to test how this new proposal fares for the even more correlated $1T$-TaS_2 [43], which is undoubtedly a known Mott insulator [14], as well as competition between CDW and SC, in future work.

ACKNOWLEDGMENTS

S.K. acknowledges Council of Scientific and Industrial Research for a senior research fellowship. M.S.L. thanks the Institut Laue-Langevin Grenoble for financial support and hospitality. We thank H. Cercellier for very helpful discussions.

APPENDIX

1. Tight-binding band structure

$TiSe_2$ is a layered material with hexagonal layers of Ti sandwiched between layers of Se atoms: a $1T$-polytype transition-metal dichalcogenide. The Ti d band is in a d^0 state in $TiSe_2$. Due to octahedral coordination, the Ti atom d shell is split into a set of high-energy e_g orbitals and low-lying, degenerate t_{2g} orbitals. We consider only the low-lying t_{2g} orbitals for they are the ones that form the hybridized bands with Se p orbitals close to the Fermi level. In the LCAO calculation, therefore, we consider charge transfer between them and the surrounding Se $4p$ orbitals, so that six Se p orbitals and three Ti d orbitals per unit cell are involved. Our results are similar to those of Wezel *et al.* [11], but we do not invoke quasi-1D features resulting from the orbital dependence of the hopping matrix elements as the driving cause of CDW. However, the shape of the central pocket around the Γ point in the DMFT Fermi surface in the main text does hint toward such anisotropic features getting more pronounced in the CDW ordered phase.

The tight-binding Hamiltonian is thus constructed as

$$\begin{aligned}\hat{H} = &\sum_{i,\alpha}\frac{\Delta}{2}(\hat{d}^{\dagger}_{i,\alpha}\hat{d}_{i,\alpha} - \hat{p}^{\dagger}_{1i,\alpha}\hat{p}_{1i,\alpha} - \hat{p}^{\dagger}_{2i,\alpha}\hat{p}_{2i,\alpha})\\ &+ \sum_{\langle i,j\rangle,\alpha,\beta}\big(t^{dd}_{\alpha,\beta,i-j}\hat{d}^{\dagger}_{i,\alpha}\hat{d}_{j,\beta}\\ &+ t^{pp}_{\alpha,\beta,i-j}[\hat{p}^{\dagger}_{1i,\alpha}\hat{p}_{1j,\beta} - \hat{p}^{\dagger}_{2i,\alpha}\hat{p}_{2j,\beta}]\big)\\ &+ \sum_{\langle i,j\rangle,\alpha,\beta}\big(t^{pd}_{\alpha,\beta,i-j}[\hat{d}^{\dagger}_{i,\alpha}\hat{p}_{1j,\beta} + \hat{d}^{\dagger}_{i,\alpha}\hat{p}_{2j,\beta} + \text{H.c.}]\\ &+ t^{pp}_{\alpha,\beta,i-j}[\hat{p}^{\dagger}_{1i,\alpha}\hat{p}_{2j,\beta} + \text{H.c.}]\big). \qquad \text{(A1)}\end{aligned}$$

Here, $\hat{d}^{\dagger}_{i}$, $\hat{p}^{\dagger}_{1i}$, and $\hat{p}^{\dagger}_{2i}$ create electrons on the Ti, the upper Se, and the lower Se atoms, respectively. The labels α and β run over all possible orientations of the Ti d-t_{2g} and Se p orbitals and $\langle i,j\rangle$ denotes neighboring sites. t^{dd}, t^{pp}, and t^{pd} are the different hopping matrices for d and p orbitals and Δ is the chemical potential.

This Hamiltonian results in a 9×9 matrix using Slater-Koster integrals, and several matrix elements vanish rigorously due to crystal symmetry. We obtain the LCAO band structure by diagonalizing the resultant matrix. By adjusting the values of Slater-Koster integrals and the chemical potential, the tight-binding bands can be fit to the extant LDA calculation. The calculated matrix elements are as follows:

$$\begin{aligned}
\epsilon 11 &= 1.0 + (9dd\sigma + 4dd\pi + 3dd\delta)\cos(x/2)\cos(\sqrt{3}y/2)/4 + 2dd\pi(\cos x),\\
\epsilon 12 &= 0,\\
\epsilon 13 &= 0,\\
\epsilon 14 &= pd\pi/4\sqrt{3}[2\cos(x/2)\cos(y/2\sqrt{3}) - 2i\cos(0.5x)\sin(y/2\sqrt{3})] - pd\pi[\cos(-y/\sqrt{3}) - i\sin(-y/\sqrt{3})]/\sqrt{3},\\
\epsilon 15 &= 5pd\pi[-2i\cos(y/2\sqrt{3})\sin(x/2) - 2\sin(x/2)\sin(y/2\sqrt{3})]/12,\\
\epsilon 16 &= -pd\pi/2\sqrt{3}\sqrt{2/3}[-2i\cos(y/2\sqrt{3})\sin(x/2) - 2\sin(x/2)\sin(y/2\sqrt{3})],\\
\epsilon 17 &= -pd\pi/4\sqrt{3}[2\cos(x/2)\cos(y/2\sqrt{3}) + 2i\cos(x/2)\sin(y/2\sqrt{3})] + pd\pi[\cos(y/\sqrt{3}) - i\sin(y/\sqrt{3})]/\sqrt{3},\\
\epsilon 18 &= 5pd\pi[-2i\cos(y/2\sqrt{3})\sin(x/2) + 2\sin(x/2)\sin(y/2\sqrt{3})/12,\\
\epsilon 19 &= -pd\pi/2\sqrt{3}\sqrt{2/3}[-2i\cos(y/2\sqrt{3})\sin(x/2) + 2\sin(x/2)\sin(y/2\sqrt{3})],\\
\epsilon 22 &= 0.9 + (3dd\pi + dd\delta)\cos(x/2)\cos(\sqrt{3}y/2) + 2dd\delta(\cos x),\\
\epsilon 23 &= -\sqrt{3}(dd\pi - dd\delta)\sin(x/2)\sin(\sqrt{3}y/2),\\
\epsilon 24 &= -pd\pi/2\sqrt{3}\sqrt{2/3}[-2i\cos(y/2\sqrt{3})\sin(x/2) - 2\sin(x/2)\sin(y/2\sqrt{3})],\\
\epsilon 25 &= 5pd\pi\sqrt{2/3}[2\cos(x/2)\cos(y/2\sqrt{3}) - 2i\cos(x/2)\sin(y/2\sqrt{3})]/6 + \sqrt{2/3}pd\pi[\cos(-y/\sqrt{3}) - i\sin(-y/\sqrt{3})]/3,\\
\epsilon 26 &= -pd\pi/2\sqrt{3}[2\cos(x/2)\cos(y/2\sqrt{3}) - 2i\cos(x/2)\sin(y/2\sqrt{3})] - pd\pi[\cos(-y/\sqrt{3}) - i\sin(-y/\sqrt{3})]/\sqrt{3})/3,\\
\epsilon 27 &= -pd\pi/2\sqrt{3}\sqrt{2/3}[-2i\cos(y/2\sqrt{3})\sin(x/2) + 2\sin(x/2)\sin(y/2\sqrt{3})],\\
\epsilon 28 &= -5pd\pi\sqrt{2/3}[2\cos(x/2)\cos(y/2\sqrt{3}) + 2i\cos(x/2)\sin(y/2\sqrt{3})]/6 - pd\pi\sqrt{2/3}[\cos(y/\sqrt{3}) - i\sin(y/\sqrt{3})]/3,\\
\epsilon 29 &= -pd\pi/2\sqrt{3}[2\cos(x/2)\cos(y/2\sqrt{3}) + 2i\cos(x/2)\sin(y/2\sqrt{3})] - pd\pi[\cos(y/\sqrt{3}) - i\sin(y/\sqrt{3})]/\sqrt{3})/3,\\
\epsilon 33 &= 0.9 + (dd\pi + 3dd\delta)\cos(x/2)\cos(\sqrt{3}y/2) + 2dd\pi(\cos x),\\
\epsilon 34 &= pd\pi/2\sqrt{2/3}[2\cos(x/2)\cos(y/2\sqrt{3}) - 2i\cos(x/2)\sin(y/2\sqrt{3})] + \sqrt{2/3}pd\pi[\cos(-y/\sqrt{3}) - i\sin(-y/\sqrt{3})],\\
\epsilon 35 &= -pd\pi/2\sqrt{3}\sqrt{2/3}[-2i\cos(y/2\sqrt{3})\sin(x/2) - 2\sin(x/2)\sin(y/2\sqrt{3})],\\
\epsilon 36 &= -pd\pi[-2i\cos(y/2\sqrt{3})\sin(x/2) - 2\sin(x/2)\sin(y/2\sqrt{3})]/6,\\
\epsilon 37 &= -pd\pi/2\sqrt{2/3}[2\cos(x/2)\cos(y/2\sqrt{3}) + 2i\cos(x/2)\sin(y/2\sqrt{3})] - \sqrt{2/3}pd\pi[\cos(y/\sqrt{3}) - i\sin(y/\sqrt{3})],\\
\epsilon 38 &= -pd\pi/2\sqrt{3}\sqrt{2/3}[-2i\cos(y/2\sqrt{3})\sin(x/2) + 2\sin(x/2)\sin(y/2\sqrt{3})],\\
\epsilon 39 &= pd\pi[-2i\cos(y/2\sqrt{3})\sin(x/2) + 2\sin(x/2)\sin(y/2\sqrt{3})]/6,\\
\epsilon 44 &= -\Delta + pp\sigma[\cos(x/2)\cos(\sqrt{3}y/2)] + 2pp\sigma(\cos x),\\
\epsilon 45 &= \sqrt{3}pp\sigma[-\sin(x/2)\sin(\sqrt{3}y/2)],\\
\epsilon 46 &= 0,\\
\epsilon 47 &= pp\sigma[2\cos(x/2)\cos(y/2\sqrt{3}) - 2i\cos(x/2)\sin(y/2\sqrt{3})]/6,\\
\epsilon 48 &= pp\sigma[-2\sin(x/2)\sin(y/2\sqrt{3}) - 2i\sin(x/2)\cos(y/2\sqrt{3})]/(6\sqrt{3}),
\end{aligned}$$

$$\epsilon 49 = 0,$$
$$\epsilon 55 = -\Delta + 3pp\sigma[\cos(x/2)\cos(\sqrt{3}y/2)],$$
$$\epsilon 56 = 0,$$
$$\epsilon 57 = pp\sigma[-2\sin(x/2)\sin(y/2\sqrt{3}) + 2i\sin(x/2)\cos(y/2\sqrt{3})]/(6\sqrt{3}),$$
$$\epsilon 58 = 2pp\sigma\{2\cos(x/2)\cos(y/2\sqrt{3}) - 2i\sin(y/2\sqrt{3})\cos(x/2) + [4\cos(-y/\sqrt{3}) - 4i\sin(-y/\sqrt{3})]\}/36,$$
$$\epsilon 59 = 0,$$
$$\epsilon 66 = -\Delta,$$
$$\epsilon 67 = 0,$$
$$\epsilon 68 = 0,$$
$$\epsilon 69 = 16pp\sigma[2\cos(x/2)\cos(y/2\sqrt{3}) - 2i\cos(x/2)\sin(y/2\sqrt{3}) + \cos(-y/\sqrt{3}) - i\sin(-y/\sqrt{3})]/9,$$
$$\epsilon 77 = -\Delta + pp\sigma[\cos(x/2)\cos(\sqrt{3}/2y)] + 2pp\sigma(\cos x),$$
$$\epsilon 78 = \sqrt{3}pp\sigma[-\sin(x/2)\sin(\sqrt{3}y/2)],$$
$$\epsilon 79 = 0,$$
$$\epsilon 88 = -\Delta + 3pp\sigma[\cos(x/2)\cos(\sqrt{3}y/2)],$$
$$\epsilon 89 = 0,$$
$$\epsilon 99 = -\Delta.$$

Setting $dd\sigma = -0.2$, $dd\pi = 0.2$, $dd\delta = -0.5$, $pd\pi = 0.5$, $pp\sigma = 0.4$, and $\Delta = 2.0$ we get a TB fit in good quantitative agreement with the LDA results [24,25,44].

2. Electron-phonon self-energy

To calculate electron-phonon self-energy we incorporate the procedure first used by Ciuchi *et al.* [27] (using Einstein phonons) into our multiorbital DMFT. The local intraorbital and interorbital Coulomb correlations are treated up to second-order self-consistent multiband IPT as usual. Since both Hubbard and electron-phonon interaction terms are local, their combined effect can be treated simultaneously within DMFT. Contribution of the electron-phonon coupling to electronic self-energy is given by

$$g^2 \sum_{i\omega_n} G_0(p) D_0(\omega) = g^2 \left[\frac{N_q + n_f(\zeta_p)}{ip_n + \omega_q - \zeta_p} + \frac{N_q + 1 - n_f(\zeta_p)}{ip_n - \omega_q - \zeta_p} \right], \quad \text{(A2)}$$

where $N_q = \frac{1}{e^{\beta\omega_q} - 1}$. The full Hamiltonian, including excitonic coupling of phonons, is

$$H = \sum_{k,a,b,\sigma} \left(t_k^{ab} + \epsilon_a \delta_{ab}\right) c_{ka\sigma}^\dagger c_{kb\sigma} + U \sum_{i,\mu=a,b} n_{i\mu\sigma} n_{i\mu-\sigma} + U_{ab} \sum_i n_{ia} n_{ib} + g \sum_i (c_{a\sigma}^\dagger c_{b\sigma} + \text{H.c.})(A_i^\dagger + A_i) - V \sum_i c_{b\sigma}^\dagger c_{b\sigma} (1 - c_{a\sigma}^\dagger c_{a\sigma}) + \omega_0 \sum_i A_i^\dagger A_i. \quad \text{(A3)}$$

We start with an initial ansatz for the self-energy $\Sigma_{\text{int}}(\omega) = Un + A\Sigma_0^{(2)}(\omega)$ where $\Sigma_0^{(2)}(\omega)$ is the second-order contribution of electron-electron and interband excitons coupling to A_{1g} phonons. The IPT scheme is that we calculate lattice Green's function (G_{fa}) from this full self-energy, from which the bare Green's function is found via the Dyson equation: $G_{0a}^{-1} = G_{fa}^{-1} + \Sigma_a$. Plugging this G_{0a} back into the IPT, we obtain a new estimate of $\Sigma_{0a}^{(2)}$ and this procedure is iterated to convergence.

Having both Hubbard-type and *el-ph* couplings changes the estimate of A_{ab} used in the interpolative self-energy in IPT as follows. Following usual procedure, A_{ab} is calculated from the condition that it reproduce the leading behavior of the (of the exact atomic limit) self-energy at high frequency. The leading behavior for large ω can be obtained by expanding the Green's function in a continuous fraction [45]: $G_{fa}(k,\omega) = 1/(\omega - \epsilon_{fa} - M_{1a} - \frac{M_{2a} - M_{1a}^2}{\omega + \ldots})$. Here, M_i denotes the ith-order moment of the density of states. One can compute these quantities by evaluating a commutator [46], and for the model above, $M_{2a} - M_{1a}^2 = U_{ab}^2[n_{fa}(1 - 2n_{fa}) + \langle n_{fa} n_{fb}\rangle] + g^2(n_{fa+} + n_{fa-})$. Here, n_{fa} is the number density calculated from the full Green's function $n_{fa+} = g^2 \sum_\omega [G_f(\omega + \omega_q)(N_q + n_f(\omega)]$ and $n_{fa-} = g^2 \sum_\omega [G_f(\omega - \omega_q)(N_q + n_f(-\omega)]$. From the large-frequency limit of (1), $\Sigma_{0a}^2(\omega) = U_{ab}^2 n_{0a}(1 - n_{0a}) + g^2(n_{0a-} + n_{0a+})$. Here, n_{0a} is a fictitious number density of the "bare" Green's function. Explicitly, $n_{0a+} = g^2 \sum_\omega [G_0(\omega + \omega_q)(N_q + n_f(\omega)]$ and $n_{0a-} = g^2 \sum_\omega [G_0(\omega - \omega_q)(N_q + n_f(-\omega)]$. Comparing with the exact high-frequency limit, we thus have $A_{ab} = \frac{U_{ab}^2[n_{fa}(1-2n_{fa}) + \langle n_{fa} n_{fb}\rangle] + g^2(n_{fa+} + n_{fa-})}{U_{ab}^2 n_{0a}(1-n_{0a}) + g^2(n_{0a-} + n_{0a+})}$.

Within the DMFT approximation, the phonon self-energy turns out to be $\Pi(q,\omega) = \frac{g^2 \chi_c(q,\omega)}{1 + g^2 \chi_c(q,\omega) D_0(q,\omega)}$ where $\chi_c(q,\omega)$ is the usual charge-charge response function [47] and $D_0(q,\omega)$ is the bare phonon Green's function. $\chi_c(q,\omega)$ is estimated

by a renormalized bubble contribution of the DMFT Green's functions. We ignore the irreducible vertex corrections since their contribution should be small for the small number of electrons and holes that characterize the two-band system close to an excitonic insulator/liquid regime, and is a further approximation.

[1] M. Imada *et al.*, Rev. Mod. Phys. **70**, 1039 (1998).
[2] Y. Kamihara *et al.*, J. Am. Chem. Soc. **128**, 10012 (2006).
[3] M. Imada *et al.*, J. Phys.: Condens. Matter **22**, 164206 (2010).
[4] J. A. Wilson *et al.*, Adv. Phys. **24**, 117 (1975).
[5] B. I. Halperin *et al.*, Rev. Mod. Phys. **40**, 755 (1968).
[6] N. E. Bickers, D. J. Scalapino, and R. T. Scalettar, Int. J. Mod. Phys. B **01**, 687 (1987).
[7] D. Pines, Phys. C (Amsterdam) **341-348**, 59 (2000).
[8] H. Cercellier *et al.*, Phys. Rev. Lett. **99**, 146403 (2007).
[9] A. Taraphder, S. Koley, N. S. Vidhyadhiraja, and M. S. Laad, Phys. Rev. Lett. **106**, 236405 (2011).
[10] C. Monney *et al.*, Europhys. Lett. **92**, 47003 (2010); Phys. Rev. Lett. **109**, 047401 (2012).
[11] J. van Wezel *et al.*, Europhys Lett. **89**, 47004 (2010).
[12] F. Weber, S. Rosenkranz, J.P. Castellan, R. Osborn, G. Karapetrov, R. Hott, R. Heid, K. P. Bohnen, and A. Alatas, Phys. Rev. Lett. **107**, 266401 (2011); S. V. Borisenko *et al.*, *ibid.* **100**, 196402 (2008).
[13] Dordevich *et al.*, Euro. Phys. J. B. **33**, 15 (2003).
[14] P. Fazekas and E. Tosatti, Philos. Mag. B **39**, 229 (1979).
[15] F. Wypych, Th. Weber, and R. Prins, Chem. Mater. **10**, 723 (1998).
[16] G. Li, W. Z. Hu, D. Qian, D. Hsieh, M. Z. Hasan, E. Morosan, R. J. Cava, and N. L. Wang, Phys. Rev. Lett. **99**, 027404 (2007).
[17] A. F. Kusmartseva, B. Sipos, H. Berger, L. Forro, and E. Tutis, Phys. Rev. Lett. **103**, 236401 (2009).
[18] B. Lake *et al.*, Science **291**, 1759 (2001).
[19] C. Monney *et al.*, Phys. Rev. B **81**, 155104 (2010).
[20] K. Held, G. Keller, V. Eyert, D. Vollhardt, and V. I. Anisimov, Phys. Rev. Lett. **86**, 5345 (2001).
[21] M. S. Laad, L. Craco, and E. Muller-Hartmann, Phys. Rev. Lett. **91**, 156402 (2003).
[22] A. I. Poteryaev, J. M. Tomczak, S. Biermann, A. Georges, A. I. Lichtenstein, A. N. Rubtsov, T. Saha-Dasgupta, and O. K. Andersen, Phys. Rev. B **76**, 085127 (2007).
[23] P. W. Anderson, Science **235**, 1196 (1987).
[24] J. van Wezel *et al.*, Phys. Status Solidi B **247**, 592 (2010).
[25] Y. Yoshida and K. Motizuki, J. Phys. Soc. Jpn. **49**, 898 (1980).
[26] A. Yaresko (private communication).
[27] S. Ciuchi *et al.*, Europhys. Lett. **24**, 575 (1993).
[28] S. Koley, N. Mohanta, and A. Taraphder, AIP Conf. Proc. **1461**, 170 (2012).
[29] *Quantum Physics in One Dimension*, edited by T. Giamarchi, International Series in Monographs on Physics (Oxford University Press, Oxford, UK, 2004); see also C. Bourbonnais and L. Caron, Int. J. Mod. Phys. B **05**, 1033 (1991).
[30] R. Arita and K. Held, Phys. Rev. B **72**, 201102(R) (2005).
[31] K. Rossnagel, L. Kipp, and M. Skibowski, Phys. Rev. B **65**, 235101 (2002).
[32] J. M. Tomczak and S. Biermann, Phys. Rev. B **80**, 085117 (2009).
[33] M. Fisher and J. Langer, Phys. Rev. Lett. **20**, 665 (1968).
[34] W. L. McMillan, Phys. Rev. **167**, 331 (1968).
[35] M. Civelli, M. Capone, A. Georges, K. Haule, O. Parcollet, T. D. Stanescu, and G. Kotliar, Phys. Rev. Lett. **100**, 046402 (2008).
[36] C. Monney *et al.*, New J. Phys. **12**, 125019 (2010).
[37] C. Monney *et al.*, Phys. Rev. Lett. **106**, 106404 (2011).
[38] C. S. Snow, J. F. Karpus, S. L. Cooper, T. E. Kidd, and T.-C. Chiang, Phys. Rev. Lett. **91**, 136402 (2003).
[39] M. S. Laad, S. Koley, and A. Taraphder, J. Phys.: Condens. Matter **24**, 232201 (2012).
[40] P. Ghaemi and T. Senthil, Phys. Rev. B **75**, 144412 (2007); **77**, 245108 (2008).
[41] S. Sachdev, Phys. Rev. Lett. **105**, 151602 (2010).
[42] A. Georges *et al.*, Rev. Mod. Phys. **68**, 13 (1996).
[43] B. Sipos *et al.*, Nat. Mater. **7**, 960 (2008).
[44] R. A. Jishi and H. M. Alyahyaei, Phys. Rev. B **78**, 144516 (2008).
[45] R. G. Gordon, J. Math. Phys. (NY) **9**, 655 (1968).
[46] W. Nolting and W. Borgiel, Phys. Rev. B **39**, 6962 (1989).
[47] O. Gunnarsson *et al.*, J. Phys.: Condens. Matter **20**, 043201 (2008).